Cell

The RacGAP β2-Chimaerin Selectively Mediates Axonal Pruning in the Hippocampus

Martin M. Riccomagno,[1,3] Andrés Hurtado,[2,6] HongBin Wang,[4] Joshua G.J. Macopson,[1,3] Erin M. Griner,[4] Andrea Betz,[5] Nils Brose,[5] Marcelo G. Kazanietz,[4] and Alex L. Kolodkin[1,3,*]
[1]The Solomon H. Snyder Department of Neuroscience
[2]Department of Neurology
The Johns Hopkins University School of Medicine, Baltimore, MD 21205, USA
[3]Howard Hughes Medical Institute, Chevy Chase, MD 20815, USA
[4]Department of Pharmacology, Perelman School of Medicine, University of Pennsylvania, Philadelphia, PA 19104-6160, USA
[5]Department of Molecular Neurobiology and DFG Center for Molecular Physiology of the Brain, Max Planck Institute of Experimental Medicine, Göttingen D-37075, Germany
[6]International Center for Spinal Cord Injury, Hugo W. Moser Research Institute at Kennedy Krieger, Baltimore, MD 21205, USA
*Correspondence: kolodkin@jhmi.edu
DOI 10.1016/j.cell.2012.05.018

SUMMARY

Axon pruning and synapse elimination promote neural connectivity and synaptic plasticity. Stereotyped pruning of axons that originate in the hippocampal dentate gyrus (DG) and extend along the infrapyramidal tract (IPT) occurs during postnatal murine development by neurite retraction and resembles axon repulsion. The chemorepellent Sema3F is required for IPT axon pruning, dendritic spine remodeling, and repulsion of DG axons. The signaling events that regulate IPT axon pruning are not known. We find that inhibition of the small G protein Rac1 by the Rac GTPase-activating protein (GAP) β2-Chimaerin (β2Chn) mediates Sema3F-dependent pruning. The Sema3F receptor neuropilin-2 selectively binds β2Chn, and ligand engagement activates this GAP to ultimately restrain Rac1-dependent effects on cytoskeletal reorganization. β2Chn is necessary for axon pruning both in vitro and in vivo, but it is dispensable for axon repulsion and spine remodeling. Therefore, a Npn2/β2Chn/Rac1 signaling axis distinguishes DG axon pruning from the effects of Sema3F on repulsion and dendritic spine remodeling.

INTRODUCTION

Axon pruning events facilitate the removal of ectopic or misguided axons and play key roles in neural circuit formation (Vanderhaeghen and Cheng, 2010). These exuberant axons often form synaptic connections; thus, synapse elimination usually precedes pruning (Liu et al., 2005; Low et al., 2008). Disruption of normal pruning events during neural development and circuit maturation is linked to mental illness and brain dysfunction (Johnston, 2004; Lewis and Levitt, 2002; Pardo and Eberhart, 2007; Rapoport et al., 1999). Axon pruning events include two classes based on histological findings: (1) degenerative-like axon collateral elimination in which axon fragmentation is observed and (2) retraction-like pruning, whereby axons draw back without shedding membrane fragments (Luo and O'Leary, 2005). Examples of the first class include axon remodeling in the *Drosophila* mushroom body (Lee et al., 1999) and, in mammals, cortical layer 5 axon pruning (Stanfield et al., 1982) and remodeling of retinocollicular axonal projections (McLaughlin et al., 2003; Nikolaev et al., 2009). However, the molecular mechanisms that underlie axon pruning are poorly understood.

A particularly interesting example of retraction-mediated stereotyped pruning involves the hippocampal infrapyramidal tract (IPT), also known as the infrapyramidal bundle (Bagri et al., 2003). During neural development, the IPT extends parallel to the main bundle (MB) of dentate gyrus mossy fibers. While the MB is directed to the apical dendrites of CA3 pyramidal neurons, the IPT axons make synaptic connections with basal dendrites of CA3 pyramidal neurons. During postnatal development, starting between postnatal day 20 (P20) and P30, distal IPT synapses are eliminated and IPT axons retract (Bagri et al., 2003; Liu et al., 2005). Variations in IPT length are correlated with behavioral deficits (Crusio et al., 1987; Lipp et al., 1988), and they accompany an assortment of genetic and environmental influences, including maternal alcohol consumption, perinatal hyperthyroidism, and epilepsy (Holmes et al., 1999; Lauder and Mugnaini, 1977; West et al., 1981). IPT pruning is regulated by the secreted semaphorin ligand Sema3F and its receptor complex, which includes neuropilin 2 (Npn-2) and plexin A3 (PlexA3) proteins (Bagri et al., 2003; Sahay et al., 2003), and this signaling pathway is well known for serving key roles in central nervous system (CNS) and peripheral nervous system (PNS) axon guidance events during neural development (Tran et al., 2007). A role for reverse ephrin-B signaling in IPT pruning has also been described (Xu and Henkemeyer, 2009).

Although axon pruning in the vertebrate hippocampus superficially resembles axonal repulsion, the degree of similarity between mechanisms that underlie axon pruning and repulsion remains to be elucidated. For example, do the same cytoplasmic effectors mediate axon pruning and guidance? Here, we show that repulsive axon guidance and stereotypical axonal pruning elicited by the same guidance cue result from the employment of distinct signaling mechanisms, shedding light on fundamental differences between unique modes of inhibitory influences on neuronal processes during postnatal neural development.

RESULTS

Downregulation of RacGTP Is Required for IPT Pruning

To investigate the molecular mechanisms underlying hippocampal IPT axon pruning, we first asked whether Rac, a small GTPase with established roles in the regulation of neuronal morphology, axon guidance, and actin remodeling (Hall and Lalli, 2010), is modulated by Sema3F. Treatment of either DIV14 hippocampal primary neuronal cultures or a neuroblastoma cell line that expresses Sema3F receptor components (Neuro2A cells; Figure S1A available online) with 10 nM Sema3F results in a significant decrease in the levels of activated Rac1 (Rac1-GTP) detected in cell lysates, as compared to alkaline phosphatase (AP) control treatment (Figures S1B and S1C; p = 0.0031 and p = 0.016 for Neuro2A cells and cultured hippocampal neurons, respectively). To assess Sema3F effects on the axonal pool of Rac1-GTP, we performed immunocytochemical detection of Rac/Cdc42-GTP using the p21-binding domain (PBD) of p21 protein (Cdc42/Rac)-activated kinase 1 (PAK1) (Harrington et al., 2011) following Sema3F or AP-control treatments. We observed a striking reduction of activated Rac/Cdc42 in axons when cultured hippocampal neurons were treated with Sema3F (Figures 1A–1C and S1D; p = 0.0008). Taken together, these Rho-GTPase pull-down and immunocytochemical assays suggest that Sema3F negatively regulates Rac1-GTP levels.

To determine whether Sema3F-mediated reduction in Rac-GTP levels is required in vivo for IPT pruning, we stereotactically injected dentate gyri of P20 mice with lentivirus vectors that encode either a constitutively active form of Rac1 (*RacQL*) under the control of the ubiquitin promoter followed by an internal ribosomal entry site (*IRES*) and enhanced green fluorescent protein (*EGFP*) or *EGFP* alone. This strategy results in robust expression of these transgenes in the dentate gyrus and produces strong labeling of most mossy fiber axons at P45 (Figure 1F). IPT pruning occurs normally in mice injected with the control EGFP-expressing lentivirus, with green-fluorescent-protein-positive (GFP^+) axons in the IPT retracting to 47% of the main mossy fiber bundle length at P45 (Figure 1D). However, GFP^+ IPT axons in hippocampi of mice injected with the *RacQL*-expressing lentivirus extend 78% of the main mossy fiber bundle length at P45 (Figures 1E and 1G). This defect in IPT retraction following expression of RacQL suggests that Rac inhibition is required for IPT pruning. Because previous work shows that synapses are present in the distal unpruned IPT of *Npn2*$^{-/-}$ and *PlexinA3*$^{-/-}$ mutant mice (Liu et al., 2005), we immunostained mice injected with the lentivirus expressing *RacQL* or the control lentivirus with the presynaptic marker vGlut1 to investigate whether Rac inhibition is also required for dissolution of presynaptic specializations. Interestingly, expression of *RacQL* in the dentate gyrus results in strong vGlut1 staining in distal GFP^+ IPT axons that is not observed in *EGFP*-expressing control-injected mice (Figures 1H and 1I). These results suggest that Rac inhibition is necessary for the elimination of IPT presynaptic components and axon pruning.

The RacGAP β2-Chimaerin Binds to Npn-2, Is Activated by Sema3F, and Is Expressed in the DG during IPT Pruning

Rho GTPase-activating proteins (GAPs) and Rho guanine nucleotide exchange factors (GEFs) play key roles in guidance cue signaling and axonal pruning (Bashaw and Klein, 2010; Billuart et al., 2001). We took a candidate approach to investigate the identity of Rac-GAPs with the potential to inhibit Rac in response to Sema3F signaling during IPT pruning, and we found that the Rac-GAP β2-Chimaerin (β2Chn) robustly binds to Npn2, the ligand-binding component of the Sema3F holoreceptor complex (Figure 2A). We performed coimmunoprecipitation (co-IP) experiments to investigate whether both members of the small chimaerin protein family, α2- or β2-chimaerin, bind to Npn-2. Though α2-chimaerin (αChn) also exhibits binding to Npn-2, it is at least ~5-fold weaker than β2Chn when normalized to input (Figures 2A and S2A). Weak binding of β2Chn to PlexinA3 was also detected (Figure S2A).

α- and β-Chn share 72% amino acid identity and are expressed in the developing and postnatal CNS (Yang and Kazanietz, 2007). αChn is implicated in axon guidance events downstream of ephrin receptor signaling (Beg et al., 2007; Iwasato et al., 2007; Wegmeyer et al., 2007), influences oculomotor function in humans (Miyake et al., 2008), regulates cortical neuronal migration (Ip et al., 2011), and, when overexpressed in vitro, induces dendritic pruning of dissociated hippocampal neurons (Buttery et al., 2006); however, the role of βChn during neural development is unknown. Because Npn-2 binds robustly to β2Chn, we asked whether Sema3F modulates β2Chn activity. We performed fluorescence resonance energy transfer (FRET) experiments by using a previously characterized β2Chn-cyan fluorescent protein (CFP)/Rac1-yellow fluorescent protein (YFP) probe pair that allows for direct assessment of β2Chn activation and recruitment to the cell membrane (Wang et al., 2006) (Figure 2B). Neuro2a cells expressing these fluorescent probes were treated with 10 nM Sema3F-AP or AP-control (Figures 2C and 2D). Though addition of control AP ligand elicits no change in FRET, treatment with Sema3F triggers a robust increase in Rac1-β2Chn interaction at the cell membrane ($p < 0.0001$) with no change in cytosolic FRET (Figures 2C–2E). These results demonstrate that Sema3F can induce β2Chn activation. To begin to address how Sema3F achieves this, we examined whether Sema3F regulates binding of β2Chn to Npn-2. Bath application of Sema3F onto Neuro2A cells for 20 min causes a significant reduction in the association of β2Chn with Npn-2 (Figure 2F), suggesting that Sema3F activation of β2Chn includes promotion of β2Chn release from Npn-2 to facilitate its activation at the cell membrane.

We next assessed the *βChn* temporal and spatial expression patterns during hippocampal postnatal development by using

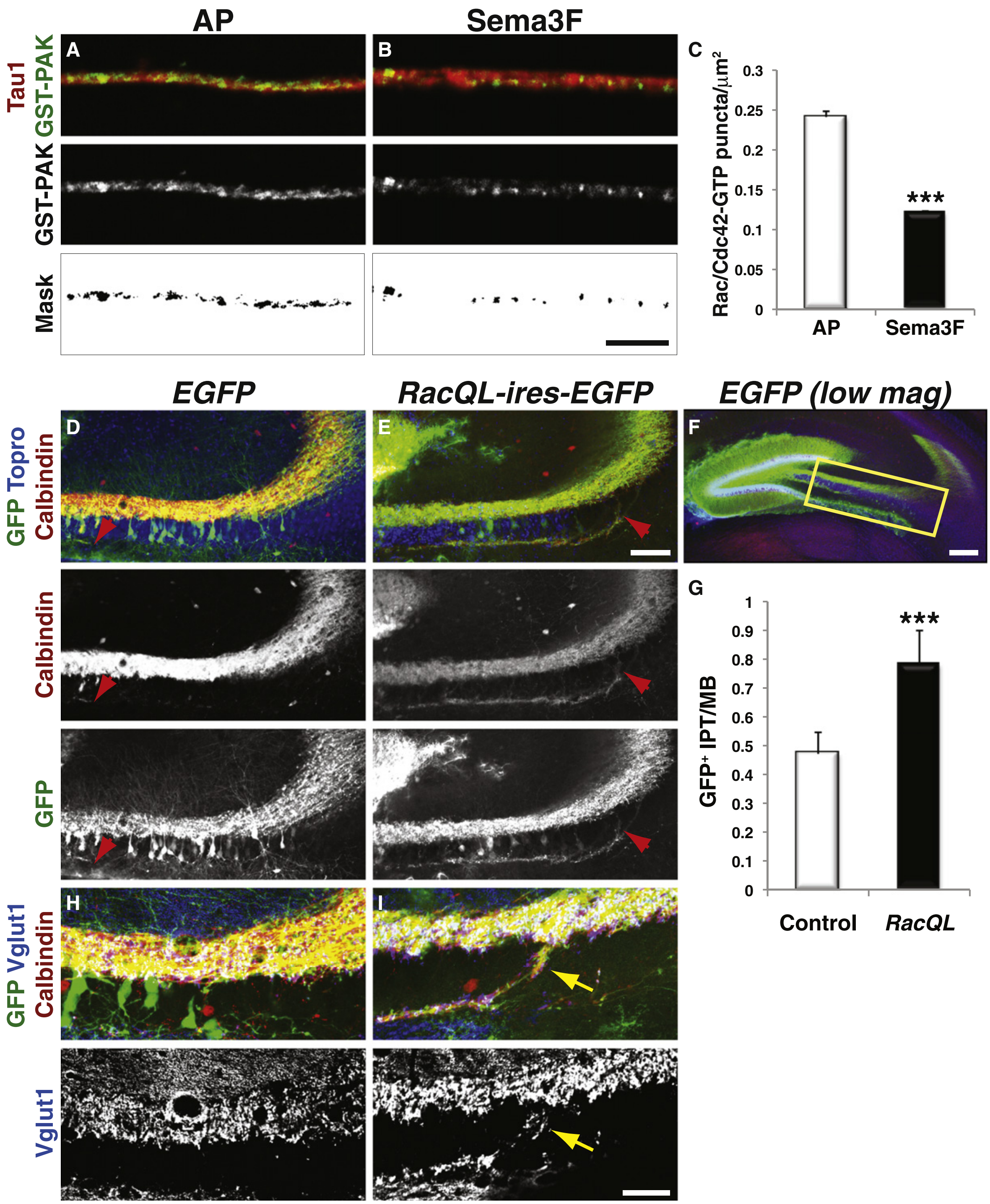

Figure 1. Downregulation of Rac-GTP Levels Is Required for Infrapyramidal Tract Pruning

(A and B) Immunostaining of DIV14 hippocampal neurons treated with 10 nM AP-control (A) or Sema3F-AP (B) by using GST-PAK1 (top, green; middle, white) and Tau1 (top, red). Bottom, black and white mask showing only GST-PAK1$^+$ puncta in Tau1$^+$ axons. Scale bar, 5 μm.

(C) Quantification of Rac/Cdc42-GTP puncta in hippocampal neurons presented as puncta per μm^2 of axonal fluorescence in AP-treated (0.24 ± 0.007 puncta/μm^2) and Sema3F-AP treated cultures (0.121 ± 0.0015 puncta/μm^2; two-tailed t test, n = 3 experiments, ***p = 0.00082).

(D–F) Expression of control *EGFP* (D and F) or *RacQL-ires-EGFP* (E) from lentivirus stereotactically injected into the dentate gyrus at P20 and shown here at P45. Coronal brain sections were immunostained for calbindin (middle, white; top, red) and GFP (bottom, white; top, green) and counterstained with ToproIII (top, blue). (E) The IPT is not pruned in the presence of constitutively active Rac. Scale bar, 100 μm. (F) GFP control lentivirus injection showing a representative region of interest magnified in (D) and (E). Red arrowheads mark the distal end of calbindin$^+$/GFP$^+$ IPT fibers. Scale bar, 250 μm.

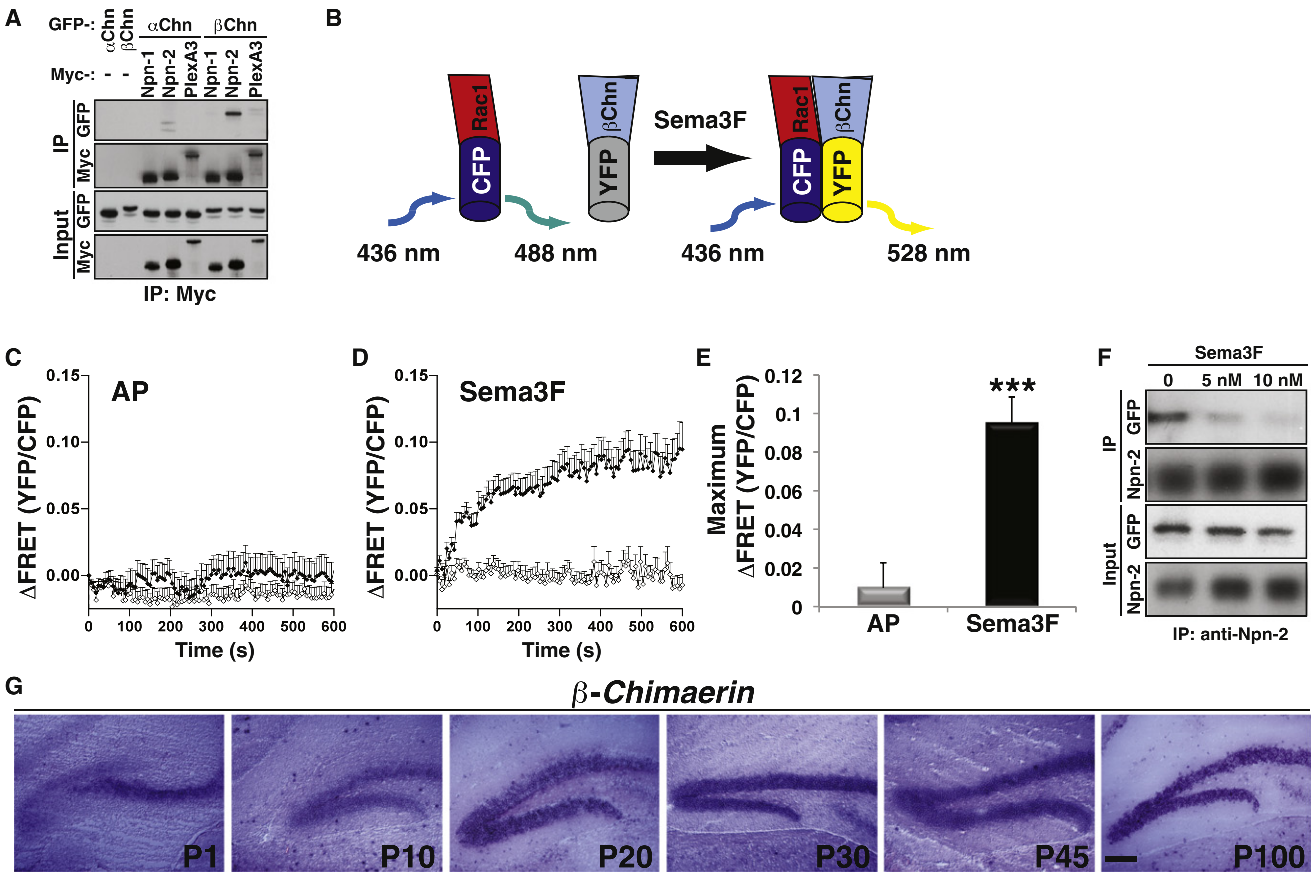

Figure 2. The Rac-GAP β2-Chimaerin Binds to Neuropilin-2 and Is Activated at the Membrane by Sema3F

(A) Coimmunoprecipitation of GFP-tagged chimaerins (α2Chn or β2Chn) with Myc-tagged neuropilin-1 (Npn-1), neuropilin-2 (Npn-2), or plexinA3 (PlexA3) in HEK293 cells in vitro. Npn-1, Npn-2, and PlexA3 were immunoprecipitated with antibodies directed against the Myc tag, and coprecipitation of chimaerins was detected. Note the strong interaction between β2Chn and Npn-2.

(B) Schematic of FRET probes used to evaluate β2Chn activation (Wang et al., 2006).

(C and D) Analysis of the β2Chn-Rac1 interaction by FRET at the membrane (full circles) or in the cytoplasm (open circles) of Neuro2A cells treated with 10 nM AP (C) or Sema3F (D). FRET was measured every 6 s after ligand treatment for 10 min. In the presence of Sema3F, a dramatic increase in FRET is observed selectively at the cell membrane, revealing that β2Chn is activated as evidenced by its binding to Rac1 and recruitment to the cell membrane. Error bars represent SEM.

(E) Quantitative analysis of maximum FRET in the peripheral region after AP or Sema3F treatment. Average maximum ΔFRET: AP, 0.0096 ± 0.013; Sema3F, 0.0944 ± 0.0141; t test, ***$p < 0.0001$; n = 34–37 membrane regions per treatment. Data are expressed as mean ±SEM.

(F) Co-IP of endogenous Npn-2 and GFP-tagged β2Chn in Neuro2A cells in the presence of different Sema3F concentrations. Npn-2 was immunoprecipitated with anti-Npn-2 and GFP-β2Chn was detected by using anti-GFP. Bath application of 5 nM and 10 nM Sema3F for 20 min causes a significant, dose-dependent reduction in β2Chn binding to Npn-2.

(G) Postnatal expression of *βChn* in the dentate gyrus assessed by in situ hybridization. *βChn* DG levels progressively increase after birth and peak during IPT pruning (P30–P45). Scale bar, 100 μm.

RNA in situ hybridization. At early postnatal stages, starting at P1, weak expression of *βChn* is observed in the dentate gyrus. However, transcript levels progressively increase and peak between P20 and P45 (Figures 2G and S2). Thus, the timing of peak *βChn* expression in the dentate gyrus overlaps with IPT pruning.

β-Chimaerin Is Required for Downregulation of RacGTP and for Presynaptic Pruning In Vitro but Is Dispensable for Axon Guidance

To test whether or not βChn, which is encoded by the *Chn2* gene, is required for Sema3F-induced inhibition of RacGTP levels, we performed immunocytochemical detection of activated

(G) Quantification of the ratio of GFP+, calbindin+ IPT length to the length of the MB in control (0.469 ± 0.07, n = 7) and *RacQL-IRES-EGFP*-injected animals (0.782 ± 0.115, n = 6, two-tailed t test: ***p = 0.00011; error bars represent SD).

(H and I) Immunostaining for vGlut1 (bottom, white; top, blue), calbindin (top, red) and GFP (top, green) in EGFP-expressing (H) or *RacQL-ires-EGFP*-expressing (I) lentivirus-injected DG granule cell axons extending within the IPT. Yellow arrows mark presynaptic vGlut1+ terminals present in *RacQL-ires-EGFP*-expressing distal IPT axons (I). Scale bar, 50 μm.

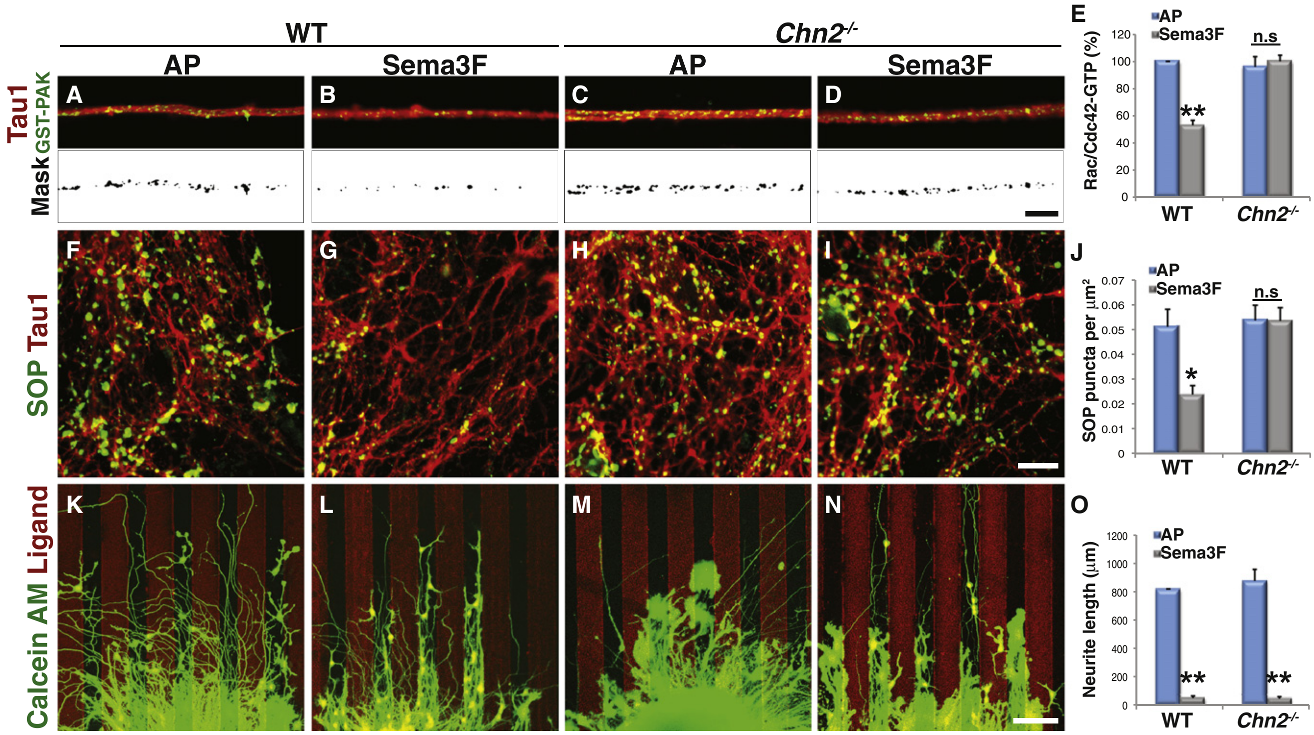

Figure 3. β2-Chimaerin Is Required for Sema3F-Dependent Pruning, but Not Repulsion, In Vitro

(A–D) WT (A and B) and *Chn2*$^{-/-}$ (C and D) hippocampal neurons were treated with 10 nM AP (control) (A and C) or Sema3F-AP (B and D) and immunostained with GST-PAK1 (top, green) and with anti-Tau1 (top, red). Bottom, mask for GST-PAK1-positive puncta in axons. Scale bar, 5 µm.

(E) Quantification of active Rac/Cdc42 in axons treated with AP or Sema3F expressed as a percentage of GST-PAK^{+} puncta/µm^2 in AP-treated WT neurons (n = 3; WT-AP, 100%; WT-Sema3F, 52.93 ± 3.63%; *Chn2*$^{-/-}$-AP, 95.95 ± 7.51%; *Chn2*$^{-/-}$-Sema3F, 100.01 ± 4.49%; ANOVA, $p < 0.0001$; Tukey HSD Test, **$p < 0.01$. Error bars represent SD).

(F–I) Synaptoporin (SOP, green) and Tau1 (red) immunolabeling of WT (F and G) and *Chn2*$^{-/-}$ (H and I) DIV21 hippocampal neurons treated with AP (F and H) or Sema3F (G and I). SOP levels are notably reduced following bath application of Sema3F to WT neurons (G), but this response is abolished in *Chn2*$^{-/-}$ neurons (I). Scale bar, 10 µm.

(J) Quantification of SOP labeling assay (n = 4 experiments, 10 fields per experiment; ANOVA, p = 0.000927, followed by Tukey HSD test, *$p < 0.05$ compared to all other treatments; error bars represent SEM). WT-AP, 0.0511 ± 0.0071; WT-Sema3F, 0.0238 ± 0.0035; *Chn2*$^{-/-}$-AP, 0.0537 ± 0.0062; *Chn2*$^{-/-}$-Sema3F, 0.0535 ± 0.0054 SOP puncta/µm^2.

(K–N) Dentate gyrus explants from P2 WT (K and L) or *Chn2*$^{-/-}$ (M and N) mice were used in stripe assays with alternating AP stripes (K and M) or alternating AP and Sema3F stripes (L and N). Both WT and *Chn2*$^{-/-}$ neurites steer away from Sema3F stripes. n = 16–20 explants per treatment, from four to five animals per genotype. Scale bar, 100 µm.

(O) Quantification of neurite outgrowth performed on WT and *Chn2*$^{-/-}$ dentate gyrus explants (see Figure S4). NS, not significant. Error bars represent SEM.

Rac/Cdc42 on wild-type (WT) and *Chn2*$^{-/-}$ hippocampal cultures acutely treated with Sema3F (Figures 3A–3D). *Chn2*$^{-/-}$ hippocampal neurons were derived from a newly generated *Chn2*$^{-/-}$ null mutant mouse (Figure S3). In contrast to the dramatic reduction in glutathione S-transferase (GST)-PAK1-PBD staining following Sema3F treatment that we observed in WT-cultured hippocampal neurons (Figures 3A, 3B, and 3E), *Chn2*$^{-/-}$ neurons show no decrease in activated Rac/Cdc42 upon Sema3F treatment (Figures 3C–3E). Because βChn is a GAP that acts specifically on Rac and does not affect the GTPase activity of Rho or Cdc42 (Yang and Kazanietz, 2007), our data demonstrate that β2Chn is required for Sema3F-dependent inhibition of Rac-GTP levels and does not significantly affect levels of activated Cdc42.

Is β2Chn required for Sema3F-induced pruning? We used an in vitro assay to address this issue. One of the first steps in IPT pruning is the disruption of previously established synaptic connections between dentate gyrus mossy fiber axons and basal dendrites of CA3 pyramidal neurons (Liu et al., 2005). To assess synapse elimination, we used the presynaptic marker synaptoporin (SOP), which specifically labels mature synaptic connections between granule cells and CA3 pyramidal neurons (Grosse et al., 1998). This allowed us to monitor the dissolution of dentate gyrus (DG)/CA3 synapses under different conditions in vitro in order to assess synapse integrity. Bath application of Sema3F onto WT cultured hippocampal neurons (21 days in vitro [DIV]) for 24 hr caused an ~50% decrease in SOP puncta, as compared to control treatment ($p < 0.01$; Figures 3F, 3G, and 3J). Although the vast majority of SOP puncta are colocalized with mossy fiber boutons (Grosse et al., 1998), a small subset of SOP puncta are associated with inhibitory synapses (Williams et al., 2011) (~25%; Figure S4A; data not shown). However, by costaining with vGlut1, we confirmed that Sema3F acts mainly to eliminate excitatory SOP$^+$;vGlut1$^+$ synapses, observing that the decrease that we see in total SOP$^+$ puncta can be attributed to the decrease in SOP$^+$/vGlut1$^+$ puncta (AP, 100 ± 10.14%; Sema3F, 40.52 ± 5.65%; $p = 9.43 \times 10^{-6}$; Figures S4A–S4F). In contrast, Sema3F treatment of *Chn2*$^{-/-}$ hippocampal neurons in culture had no effect on the number of SOP puncta, showing that β2Chn is required for Sema3F-induced elimination of granule cell MF/CA3 pyramidal neuron synapses in vitro (Figures 3H–3J).

β2Chn functions in vitro to mediate Sema3F-dependent presynaptic pruning; however, is it required for Sema3F-dependent repulsive guidance? To address this question, we cultured P2 DG explants from WT mice, which maintain expression of *β2Chn* in vitro (Figures S4G and S4H), and from *Chn2*$^{-/-}$ mice on alternating stripes of control and Sema3F-AP or AP control only (Figures 3K–3N). Control stripes had no effect on neurites extending from WT or *Chn2*$^{-/-}$ DG explants (Figures 3K and 3M). Interestingly, both WT and *Chn2*$^{-/-}$ axons steered away from Sema3F-AP stripes and extended primarily along the control stripes (Figures 3L and 3N). This shows that β2Chn is dispensable for Sema3F-dependent repulsive axon guidance, establishing that synaptic pruning and repulsive guidance in vitro are distinct with respect to a requirement for β2Chn. We also asked whether β2Chn affects sensitivity to Sema3F in neurite outgrowth assays by culturing WT and *Chn2*$^{-/-}$ DG explants in the presence of Sema3F-AP or AP control ligand. Consistent with our stripe assays, 10 nM Sema3F-AP strongly inhibited neurite outgrowth of both WT and *Chn2*$^{-/-}$ DG explants (Figures 3O and S4I–S4M). Only at a 10-fold lower concentration did Sema3F exert a somewhat stronger inhibitory effect on neurite outgrowth in WT DG explants, as compared to *Chn2*$^{-/-}$ DG explants ($p = 0.015$; Figure S4M). Taken together, these results show that β2Chn is required for Sema3F-dependent presynaptic pruning but that it is not essential for Sema3F-mediated DG axon repulsion.

β-Chimaerin Is Required and Is Sufficient for IPT Pruning

Sema3F, Npn-2, and PlexA3 are required in vivo for IPT pruning (Bagri et al., 2003; Sahay et al., 2003). Therefore, we next asked whether β2Chn is necessary for this developmental process. We performed histological analysis of WT and *Chn2*$^{-/-}$ P45 hippocampi. Timm and anti-calbindin staining show that, by P45, the IPT of WT mice is pruned to 51% of the main mossy fiber bundle length (Figures 4A, 4C, 4E, S5A, and S5A′). However, the IPT of *Chn2*$^{-/-}$ mice fails to be pruned, remaining 87% of the length of the MB (Figures 4B, 4D, 4E, S5B, and S5B′; phenotype observed with full penetrance and expressivity). We next asked whether presynaptic terminals were still present in the distal region of the *Chn2*$^{-/-}$ unpruned IPT by immunostaining for the presynaptic marker vGlut1. Although WT mice did not exhibit vGlut1$^+$ terminals at the distal portion of the region where the IPT was pruned, abundant vGlut1$^+$ puncta are found in the infrapyramidal region near the distal portion of the unpruned IPT mossy fibers in *Chn2*$^{-/-}$ mice (Figures 4C and 4D), suggesting a defect in synaptic pruning. To confirm that β2Chn is required for IPT synaptic pruning, we analyzed the distal infrapyramidal region of WT and *Chn2*$^{-/-}$ mice by using transmission electron microscopy (TEM) and quantified the number of synapses in this region (Figures 4F–4H). Consistent with the perdurance of vGlut1 staining that we observe in distal unpruned *Chn2*$^{-/-}$ IPT axons, TEM analysis of *Chn2*$^{-/-}$ mice revealed a significant increase in the number of synapses in the distal infrapyramidal region of CA3 as compared to WT (Figures 4F–4H; $p = 0.005$). Similarities in synaptic pruning phenotypes observed in *Chn2*$^{-/-}$ and *Npn2*$^{-/-}$ animals are restricted to DG IPT connections onto CA3 neurons because we find that the number of spines along DG granule cell dendrities, which is significantly increased in *Npn2*$^{-/-}$ and *Sema3F*$^{-/-}$ mice (Tran et al., 2009), is equivalent to WT in *Chn2*$^{-/-}$ mice (Figures 4I–4K). Furthermore, *Chn2*$^{-/-}$ null mutant mice do not show the embryonic trochlear and oculomotor nerve axon guidance defects or the late embryonic-postnatal anterior commissure phenotypes that are observed in *Npn2*$^{-/-}$ mice (Figures S5C–S5F) (Chen et al., 2000; Giger et al., 2000). Thus, *Chn2* is selectively required for Sema3F-mediated IPT pruning, but not for Npn-2-dependent axon guidance or dendritic spine remodeling.

Our analysis of *Chn2*$^{-/-}$ mice demonstrates a requirement for β2Chn in IPT synaptic pruning and axon retraction. To determine whether β2Chn acts in an instructive fashion to enhance IPT pruning, we took advantage of a newly generated knockin mouse that harbors an allele of *Chn2* encoding a hyperactive form of βChn; this allele consists of a single amino acid change that has been introduced into the endogenous *Chn2* locus (Figure S6). This I130A point mutation causes the βChn protein to remain in an ‘‘open’’ conformation, rendering the protein more sensitive to induction and, thus, hyperactive (Canagarajah et al., 2004). Because *Chn2*^{I130A} mice produce Chn2 protein that is more easily induced, but not constitutively active (Canagarajah et al., 2004; Yang and Kazanietz, 2007), we asked whether or not this mutation, when homozygous, enhanced pruning at P28, a postnatal time that is well after the onset of IPT pruning but prior to its completion. At P28, the length of the WT IPT is 66% of the MB length (Figures 5A and 5C). This is in contrast to the IPT in *Chn2*$^{I130A/I130A}$ mice, in which the IPT is significantly shorter at this same postnatal time point (49% of the MB length; Figures 5B and 5C). Importantly, the lengths of WT and *Chn2*$^{I130A/I130A}$ IPTs are not significantly different prior to the onset of pruning at P15 (Figures S6G–S6I). These results show that a hyperactive βChn allele enhances IPT pruning.

The IPT pruning defects observed in *Chn2*$^{-/-}$ mice closely resemble those observed in *Npn-2*$^{-/-}$, *PlexA3*$^{-/-}$, and *Sema3F*$^{-/-}$ hippocampi (Bagri et al., 2003; Liu et al., 2005; Sahay et al., 2003). We obtained additional evidence that *Npn-2* and *Chn2* act in concert during IPT development from an analysis of single and compound heterozygous mutant mice. Histological examination of *Chn2*$^{+/-}$ and *Npn-2*$^{+/-}$ mice revealed that the IPT length in either single heterozygote is indistinguishable from WT at P45 (Figures 5D and 5E). However, transheterozygous *Chn2*$^{+/-}$; *Npn-2*$^{+/-}$ P45 mice exhibit a significant increase in IPT length as compared to WT ($p < 0.01$; Figures 5D and 5E), phenocopying *Chn2*$^{-/-}$ and *Npn-2*$^{-/-}$ single homozygous null mutants (Bagri et al., 2003) (Figure 4B). This robust genetic interaction in vivo, combined with our biochemical observations, strongly suggests that Sema3F, Npn-2, and β2Chn function in a common pathway to regulate IPT pruning.

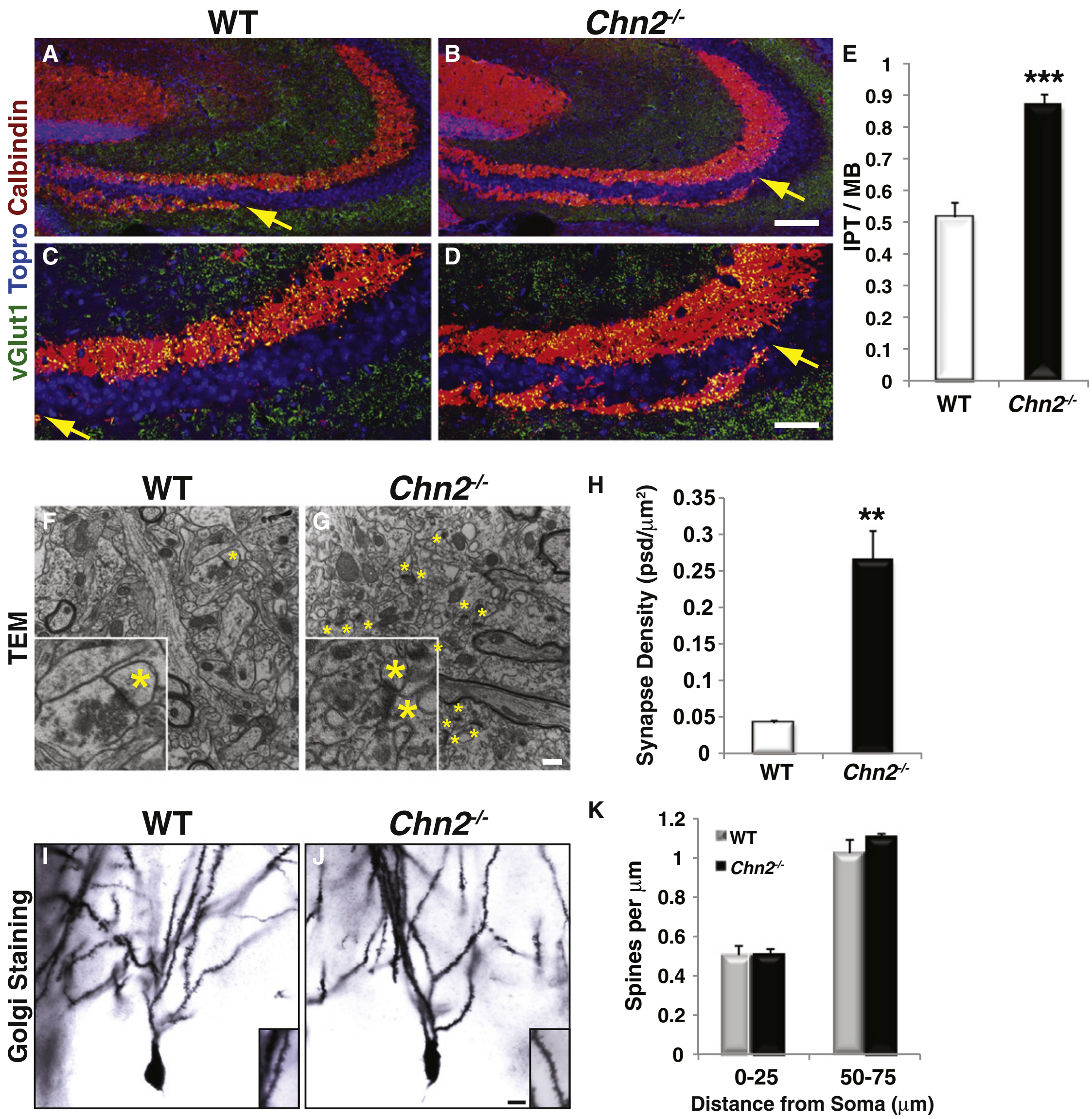

Figure 4. β2-Chimaerin Is Required for IPT Pruning In Vivo but Is Dispensable for DG Dendritic Spine Remodeling

(A–D) Immunostaining of WT (A and C) and *Chn2*$^{-/-}$ (B and D) P45 hippocampi with anti-calbindin (red), anti-vGlut1(green), and ToproIII (blue). The IPT is notably longer in *Chn2*$^{-/-}$ mice (B) compared to WT (A). Yellow arrows mark the distal end of the IPT. Scale bar, 100 μm. (C and D) Higher magnification views of (A) and (B), respectively. vGlut1^{+} presynaptic terminals are observed in the distal region of the IPT in *Chn2*$^{-/-}$ mice (D). Scale bar, 50 μm.

(E) Quantification of IPT pruning, expressed as the ratio of IPT length to the length of the MB in CA3. The IPT is significantly longer in *Chn2*$^{-/-}$ mice (0.87 ± 0.034; n = 12 brain hemispheres from eight mutant mice) than in WT (0.515 ± 0.046; n = 13 hemispheres from eight WT mice; two-tailed t test, ***p = 8.02*10^{-17}; error bars represent ±SD).

(F and G) Transmission electron micrographs of distal IPT regions in WT (F) and *Chn2*$^{-/-}$ (G) mice. Insets show a single axon terminal and postsynaptic density (PSD) in WT (F) and a characteristic mossy fiber asymmetric synapse with two PSDs in *Chn2*$^{-/-}$ (G) mice. Asterisks mark PSDs. Scale bar, 500 nm for (F) and (G), and 150 nm for insets.

(H) Quantification of synapses in the distal infrapyramidal region of WT and *Chn2*$^{-/-}$ mice determined from electron microscopy (EM) analysis. WT, 0.042 ± 0.003 psd/μm^2; *Chn2*$^{-/-}$, 0.265 ± 0.069 psd/μm^2; two-tailed t test, **p = 0.005, error bars represent SEM.

(I and J) *Chn2* is not required for DG granule cell dendritic spine or anterior commissure development. Golgi staining of adult DG granule cell dendrites in WT (I) and *Chn2*$^{-/-}$ (J) hippocampi. Scale bar, 10 μm for (I) and (J) and 6 μm for insets.

(K) Quantification of WT and *Chn2*$^{-/-}$ DG granule cell dendritic spine density; no significant difference between WT and *Chn2*$^{-/-}$ is observed (t test, p = 0.83 for 0–25 μm and p = 0.11 for 50–75 μm; error bars represent ±SD).

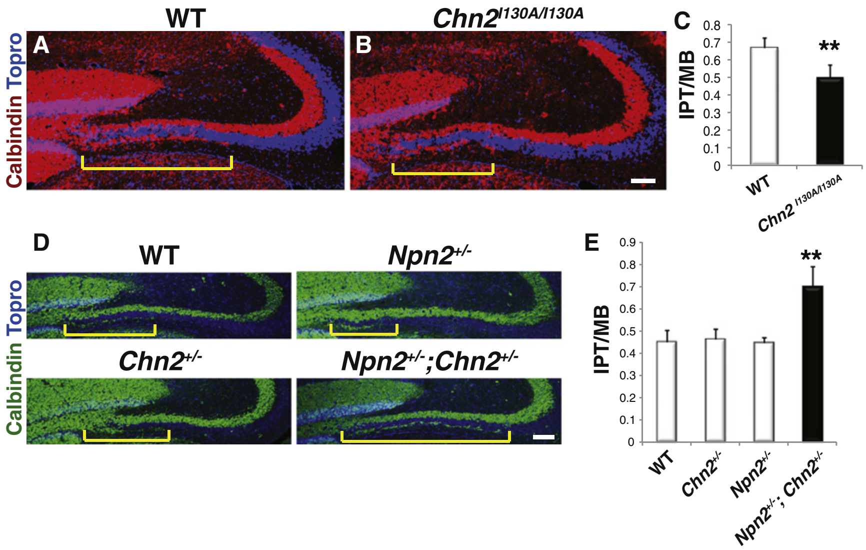

Figure 5. A Hyperactive Form of β-Chimaerin Is Sufficient for IPT Pruning In Vivo

(A and B) Immunohistochemistry with anti-calbindin (red) and ToproIII (blue) on WT and *Chn2*$^{I130A/I130A}$ P28 hippocampi. Scale bar, 100 μm.

(C) Quantification of the IPT length-to-MB length ratio in WT (0.664 ± 0.057) and *Chn2*$^{I130A/I130A}$ (KI/KI) mice (0.495 ± 0.072; n = 8; two-tailed t test, **p = 0.00596).

(D and E) Genetic interaction between *Npn-2* and *Chn2*. (D) Immunostaining using anti-calbindin (green) and ToproIII (blue) of WT (top left), *Npn-2*$^{+/-}$ (top right), *Chn2*$^{+/-}$ (bottom left), and *Chn2*$^{+/-}$; *Npn2*$^{+/-}$ transheterozygotes (bottom right) P45 hippocampi. Scale bar, 100 μm. (E) Quantification of the genetic interactions between *Chn2* and *Npn2* (n = 7 hemispheres from five animals for each genotype; ANOVA, p < 0.0001; Tukey HSD test, **p < 0.01 compared to all other genotypes). WT, 0.45 ± 0.053; *Chn2*$^{+/-}$, 0.463 ± 0.046; *Npn-2*$^{+/-}$, 0.447 ± 0.024; *Chn2*$^{+/-}$; *Npn2*$^{+/-}$, 0.698 ± 0.092. Yellow brackets delineate IPT length in (A), (B), and (D). Error bars represent SD.

DG-Autonomous Requirement for β2-Chimaerin and Its GAP Activity during IPT Pruning

To ask whether βChn is indeed required in DG granule cells to mediate IPT pruning, a series of short hairpin RNAs (shRNAs) were generated by using the pLEMPRA system (Zhou et al., 2006) to knock down *Chn2* cell type autonomously in DG granule cells. Two of several shRNAs tested (*shRNA2* and *shRNA4*) elicited significant downregulation of β2Chn expression (Figure S7; data not shown). *shRNA2* is predicted to anneal to and downregulate transcripts encoding only one of the two known βChn isoforms, β2Chn (which contains the SH2 domain); however, *shRNA4* downregulates the expression of transcripts encoding both the β1Chn isoform (which does not contain the SH2 domain) and the β2Chn isoform (Yang and Kazanietz, 2007). We generated lentiviruses that express both *shRNA2* and *shRNA4*, stereotactically injected them into the DG at P20, and then analyzed the IPT at P45 (Figure 1F). Injection of an EGFP-expressing control lentivirus had no effect on IPT pruning (Figures 6A and 7C). Injection of lentiviruses expressing either *shRNA2* or *shRNA4*, however, resulted in a robust GFP^{+} IPT pruning defect (p < 0.01; Figures 6B, 6C, and 7C). Therefore, βChn is required in DG granule cells to regulate IPT pruning. Further, these results also confirm that the isoform of βChn essential for IPT pruning is β2Chn; *shRNA2* only knocks down β2Chn. However, *shRNA4* knocks down both isoforms of *βChn*, and we find that both shRNAs elicit the same infrapyramidal tract pruning defect (Figures 6B, 6C, and 7C). To rule out the possibility that these defects observed in *shRNA2*-injected animals are due to off-target shRNA effects and also to show that this shRNA acts specifically to silence *β2Chn*, we generated a pLEMPRA rescue construct that expresses both *shRNA2* and the WT human form of *β2Chn* (*WT**), which is insensitive to *shRNA2* (Figure S7). Injection of the *shRNA2+WT** lentivirus completely rescues the IPT pruning phenotype observed in *shRNA2*-injected animals (Figures 7A and 7C), demonstrating that *shRNA2* acts specifically on *β2Chn* and that β2Chn is required for IPT axon pruning.

Analysis of *Chn2*$^{-/-}$ mice revealed a requirement for β2Chn in IPT axonal and presynaptic pruning. To investigate whether βChn is required in DG granule cells for dissolution of IPT synaptic specializations, we performed vGlut1 immunostaining of control-, *shRNA2*-, and *shRNA4*-injected hippocampi (Figures 6D–6F). Indeed, vGlut1 staining is absent from the distal infrapyramidal region of mossy fibers in control EGFP-expressing lentivirus-injected animals (Figure 6D). However, both *shRNA2*- and *shRNA4*-injected animals show strong vGlut1immunolabeling on distal GFP^{+} IPT axons (Figures 6E and 6F), showing that βChn is required in DG granule cells to regulate IPT mossy fiber presynaptic elimination. Injection of *shRNA2+WT** lentivirus completely rescues the perdurance of the presynaptic marker vGlut1 that is observed in *shRNA2*-injected animals (Figures 6E and 7D), further confirming the specificity of the *shRNA2* knockdown and the requirement for β2Chn in IPT axon and presynaptic pruning.

We observe that Sema3F downregulates Rac-GTP in DG neurons and that constitutively active Rac blocks IPT pruning in vivo (Figure 1). In addition, our in vitro observations using *Chn2*$^{-/-}$ neuronal cultures show that β2Chn is required for Sema-3F-mediated downregulation of Rac-GTP (Figures 3A–3E). These observations suggest that β2Chn Rac-GAP activity is required for IPT pruning. To test this hypothesis, we generated a pLEMPRA rescue construct expressing human β2Chn (which is insensitive to *shRNA2*) that harbors a microdeletion in the β2Chn GAP domain, rendering it inactive (Siliceo et al., 2006) (*shRNA2+ΔEIE**; Figure S7). Expression levels of *shRNA2+WT** and *shRNA2+ΔEIE** lentiviruses are similar (Figure S7). In contrast to the complete rescue observed when *shRNA2+WT** lentivirus was injected into the DG, *shRNA2+ΔEIE**-injected animals exhibited exuberantly extended GFP^{+} IPT axons that were significantly longer than the IPTs of control- or *shRNA2+WT**-injected animals (p < 0.01; Figures 6A and 7A–7C). Closer examination of distal GFP^{+} IPT fibers in *shRNA2 + ΔEIE**-injected animals revealed extensive vGlut1 immunostaining (Figure 7E), indicating that presynaptic elimination also

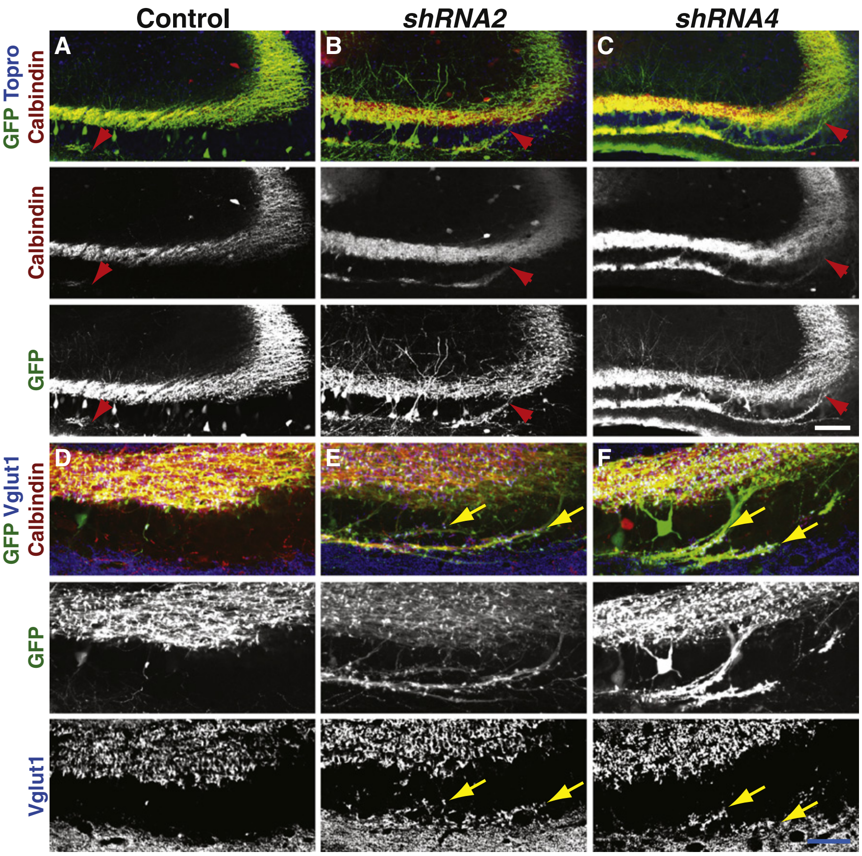

Figure 6. β2Chn Is Required in the Dentate Gyrus for IPT Pruning In Vivo

(A–C) Histological analysis of hippocampi from control (A), *shRNA2* (B), and *shRNA4* (C) lentivirus-injected animals using anti-GFP (top, green; bottom, white), anti-calbindin (top, red; middle, white), and ToproIII (top, blue). The IPT in *shRNA2*- and *shRNA4*-injected animals (B and C) extends almost as far as the distal blade of the MB, as compared to control-injected animals in which the IPT extends only 45% of the MB length (A). Arrowheads mark the distal end of the calbindin$^+$, GFP$^+$ IPT fibers. Scale bar, 100 μm.

(D–F) β2-chimaerin is required in the dentate gyrus for IPT presynaptic pruning. Immunostaining for vGlut1 (bottom, white; top, blue), calbindin (top, red), and GFP (middle, white; top, green) of control (D), *shRNA2* (E), and *shRNA4* (F) lentivirus-injected mice. Ectopic vGlut1$^+$ presynaptic terminals are present in the distal region of the IPT in *shRNA*-injected hippocampi (E and F). Arrows point to presynaptic vGut1$^+$ terminals present in shRNA-injected EGFP$^+$ distal IPT axons. Scale bar, 50 μm.

requires an active β2Chn GAP domain. These results show that β2Chn Rac-GAP activity is required in vivo for IPT presynaptic elimination and axon pruning.

DISCUSSION

We demonstrate here that Sema3F-dependent inhibition of Rac1 by the Rac-GAP β2Chn is required for hippocampal infrapyramidal tract pruning. Axon pruning and other neural developmental processes, including axon guidance, synapse remodeling, and dendritic spine elimination, play essential roles during the establishment of functional brain circuitry (Vanderhaeghen and Cheng, 2010). Although little is known about the signaling pathways that regulate axon pruning, recent studies have uncovered mechanisms that regulate degenerative-like axon elimination, highlighting the importance of signaling pathways previously shown to mediate controlled cell death (Nikolaev et al., 2009), proteasome-mediated degradation (Watts et al., 2003), and Wallerian degeneration (Hoopfer et al., 2006). Our observations provide insight into the molecular mechanisms that regulate stereotyped retraction-mediated axon pruning. They support a role for Sema3F-mediated activation of the Rac-GAP β2Chn in stereotyped axon pruning and synapse elimination in the IPT, a hippocampal tract implicated in spatial memory and avoidance learning (Crusio et al., 1987; Lipp et al., 1988).

RhoGTPase-Mediated Signaling and Stereotyped Axon Pruning

Our data support a model in which Sema3F signaling activates a RacGAP in order to downregulate RacGTP levels, thereby promoting presynaptic remodeling and axon pruning. Treatment of hippocampal neuronal cultures with Sema3F causes a significant decrease in axonal RacGTP levels. Overexpressing a constitutively active form of Rac prior to the onset of IPT pruning results in a lack of IPT axon retraction and synapse elimination, revealing that downregulation of RacGTP is critical for IPT pruning in vivo. Whereas Rac inhibition by Sema3F is required in vitro and in vivo for hippocampal IPT pruning, ephrin reverse signaling, which is essential for IPT pruning in vivo, activates Rac1 in vitro by recruiting the adaptor protein Grb4 and the RacGEF Dock180 (Xu and Henkemeyer, 2009). This raises the possibility that tight temporal and spatial regulation of Rac activation and inactivation, provided by opposing activities of Sema3F and ephrin reverse signaling, may be important for IPT pruning. Assessment of crosstalk between these two signaling pathways in vivo will further our understanding of the molecular mechanisms that underlie IPT pruning. Whether regulation of Rho GTPases is a common feature of retraction-like and degradation-mediated pruning remains to be elucidated. In that regard, p190RhoGAP is required for the regulation of *Drosophila* mushroom body remodeling, a degeneration-like pruning event (Billuart et al., 2001), and this raises the possibility that these two classes of pruning, although superficially distinct, may share common molecular mechanisms. Future experiments will determine whether similar signaling events underlie other classes of axon pruning in mammals.

How does Sema3F regulate β2Chn activity? Genetic and biochemical evidence suggest that Npn-2 and β2Chn act in

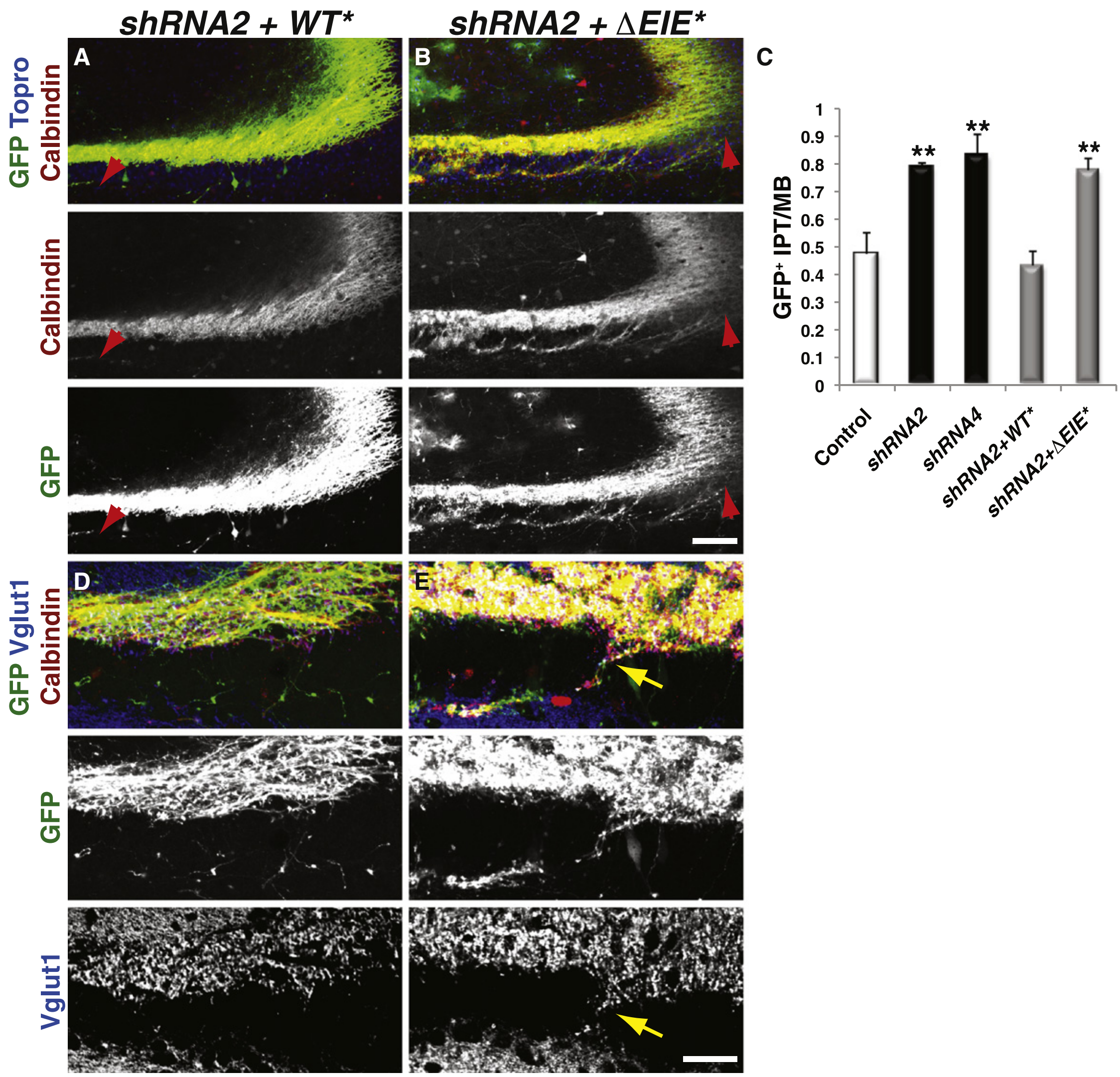

Figure 7. β2Chn GAP Function Is Required in the Dentate Gyrus for IPT Pruning In Vivo

(A and B) Immunostaining of hippocampal sections obtained from *shRNA2*+WT* (A) and *shRNA2*+Δ*EIE** (B) lentivirus-injected animals using anti-GFP (top, green; bottom, white), anti-calbindin (top, red; middle white), and ToproIII (top, blue). The defect observed in shRNA-injected animals (see Figure 6) can be rescued by human WT β2Chn (A), but not by a human β2Chn harboring a three-amino-acid deletion rendering the GAP domain inactive (ΔEIE, B). Arrowheads mark the distal end of the calbindin$^+$, GFP$^+$ IPT fibers. Scale bar, 100 μm.

(C) Quantification of GFP$^+$, calbindin$^+$ IPT length expressed as a ratio of IPT/MB length. Control, 0.47 ± 0.07, n = 7; *shRNA2*, 0.78 ± 0.013, n = 6; *shRNA4*, 0.83 ± 0.07, n = 5; *shRNA2+WT**, 0.43 ± 0.06, n = 9; *shRNA2+ΔEIE**, 0.77 ± 0.04, n = 6. ANOVA ($p < 0.0001$) followed by Tukey HSD test, **$p < 0.01$ compared to control and *shRNA2+WT**; error bars represent ±SD.

(D and E) The Rac-GAP activity of β2Chn is required in the dentate gyrus for IPT presynaptic pruning. Immunohistochemistry for vGlut1 (bottom, white; top, blue), calbindin (top, red) and GFP (middle, white; top, green) of *shRNA2+WT** (D) and *shRNA2+ΔEIE** (E) lentivirus-injected mice. Injection of human *shRNA*-resistant WT *β2-Chimaerin* rescues the accumulation of vGlut1 in the distal IPT region (D); however, a human GAP-deficient form of β2-Chimaerin (ΔEIE) (E) fails to rescue the IPT pruning defect observed in *shRNA*-injected hippocampi. Arrows point to presynaptic vGut1$^+$ terminals present in shRNA-injected EGFP$^+$ distal IPT axons (E). Scale bar, 50 μm.

concert to direct IPT pruning. Interestingly, Sema3F promotes dissociation of β2Chn from Npn-2 in a dose-dependent manner. One plausible scenario is that Sema signaling acts in a sequential, ligand-gated manner to regulate β2Chn activation. Npn-2 recruits and sequesters β2Chn in relevant areas of the cell, for example, in close proximity to the axonal membrane. Sema3F binding to Npn-2 then promotes the release of β2Chn, which initiates pruning through subsequent recruitment to the membrane and activation.

Semaphorin signaling is essential for IPT pruning and the synapse elimination events that precede it (Liu et al., 2005). Histological evidence reveals that, in *Npn-2*$^{-/-}$ and *PlexA3*$^{-/-}$ mice, synapse elimination and IPT pruning do not occur because exuberant axons and synaptic terminals remain in the distal IPT region of these mutants (Liu et al., 2005). We find that β2Chn function and downregulation of RacGTP are also required for both of these developmental processes. It remains to be seen whether synapse elimination and IPT axonal pruning are two distinct and sequential cellular events or whether both developmental processes are intrinsically linked and controlled by the same molecular mechanisms. Because *Chn2*, *Sema3F*, *Npn-2*, and *PlexA3* mouse null mutants show defects in IPT axon pruning and synapse elimination (Liu et al., 2005) (Figure 4), it seems likely that both events are tightly coupled and regulated in a similar fashion.

Unbalanced synaptic and axonal pruning is implicated in the etiology of mental illness (Johnston, 2004; Lewis and Levitt, 2002; Pardo and Eberhart, 2007; Rapoport et al., 1999; Vanderhaeghen and Cheng, 2010). Improper regulation of axon and synaptic pruning in the cortex, cerebellum, and limbic system is correlated with increases in white matter and has been linked to epilepsy and autism (Johnston, 2004; Pardo and Eberhart, 2007; Vanderhaeghen and Cheng, 2010). Furthermore, excessive cortical neurite and synaptic pruning during puberty is correlated with the early onset of schizophrenia (Lewis and Levitt, 2002; Rapoport et al., 1999). Interestingly, a missense polymorphism identified in the human gene that encodes βChn, which results in the change of a highly conserved histidine residue to arginine (H204R), is genetically linked to schizophrenia (Hashimoto et al., 2005). Future experiments will address whether βChn plays any role in the etiology of schizophrenia and related disorders.

Selective Requirement for β2Chn during Axonal Pruning

It is intriguing that, although β2Chn is required for Sema3F-dependent IPT pruning, this RacGAP is apparently dispensable for Sema3F-mediated DG axon repulsion and dendritic spine remodeling. Indeed, *β2Chn* mutants do not exhibit any of the axon guidance or dendritic morphology defects associated with null mutations in *Sema3F*, *Npn-2*, or *PlexA3* (Figure S5; data not shown) (Chen et al., 2000; Giger et al., 2000; Sahay et al., 2003; Tran et al., 2009). β2Chn may confer unique signaling properties required for pruning by increasing the "gain," or sensitivity, of granule cell axons to Sema3F signaling involving the same signaling pathways required for regulating neuronal morphology and process guidance. Alternatively, β2Chn may activate signaling pathways that are vital for Sema3F-mediated axon pruning but are distinct from those utilized by Sema3F-mediated axonal repulsion and dendritic spine remodeling. Rather than exclusive utilization of one particular signaling pathway, a balance between different regulators may be required for distinct neuronal responses to extrinsic cues. The differential requirement for β2Chn in axon pruning, but not axon guidance or dendritic spine remodeling, is one of the first mechanistic distinctions identified among these three developmental inhibitory processes, which, in this case, are all mediated by the same guidance cue. Determining the signaling context in which Rho GTPase regulation governs axon pruning and whether neuronal process pruning and synapse elimination in other neural systems utilize similar mechanisms to sculpt mature neural circuits will shed light on the underlying mechanisms that participate in neuronal remodeling.

EXPERIMENTAL PROCEDURES

Generation of Transgenic Animals

The mouse line carrying a targeted deletion for *β2-chimaerin* ($Chn2^{-/-}$) was generated by using the knockout (KO)-vector pFlexHR (Schnütgen et al., 2003) and results in the abrogation of β2-chimaerin protein expression with concomitant expression of a lacZ cassette under the control of the *Chn2* gene promoter (Figure S3). The knockin mouse carrying the hyperactive mutant *I130A-β2-chimaerin* was generated by using the targeting vector pTKNeoLox (Fernández-Chacón et al., 2001).

Stereotactic Injection of Lentiviruses

Concentrated viral solution (1 μl), prepared as previously described (Lois et al., 2002), was delivered into the DG by stereotactic injection (0.25 μl per min). For P20 mice, we used the following coordinates: anterior-posterior, –2.1 mm; lateral, ±1.7 mm; and vertical, –1.9 mm. For all injections, Bregma was the reference point.

Fluorescence Resonance Energy Transfer

Neuro-2a cells were transfected with CFP-Rac1 (WT) and YFP-β2-chimaerin (WT) by using Metafectene PRO (Biontex, Germany); serum-free and phenol-red-free medium (10 mM HEPES) was added 24 hr after transfection. Images (exposures of 500 ms) were taken every 6 s after the addition of either Sema3F (10 nM) or AP (10 nM), and FRET analysis was performed as previously described (Wang et al., 2006).

Statistical Analysis

Quantitation of IPT retraction was performed by using the ratio of IPT length to the length of the MB. IPT and MB length were measured from the tip of the inferior blade of the dentate granule cell layer, as reported previously (Bagri et al., 2003). Statistical differences for mean values between two samples were determined by two-tailed Student's t test for independent samples. Statistical analyses among multiple groups were determined by using analysis of variance (ANOVA) followed by Tukey's multiple comparison test. The criterion for statistical significance was set at $p < 0.05$.

Tissue Culture and Immunohistochemistry

Hippocampal neuronal cultures were generated as previously described (Tran et al., 2009). Immunohistochemistry and in situ hybridization were performed as previously described (Giger et al., 2000).

SUPPLEMENTAL INFORMATION

Supplemental Information includes Extended Experimental Procedures and seven figures and can be found with this article online at doi:10.1016/j.cell.2012.05.018.

ACKNOWLEDGMENTS

We thank Dr. Silvio Gutkind for the *RacQL* construct, Barbara Smith and the JHU School of Medicine Microscope Facility for assistance with the TEM, and Dr. Michael Greenberg for the pLLX and pLEMPRA vectors. We also thank Drs. Cynthia Duggan, Roman Giger, David Ginty, Randal Hand, Kang Shen, and Marc Tessier-Lavigne for helpful comments on the manuscript and discussions, and we thank members of Kolodkin laboratory for assistance. This work was supported by a postdoctoral fellowship from the National Ataxia Foundation to M.M.R, NIH R01 CA74197 to M.G.K, and NIH RO1 MH59199 to A.L.K. A.L.K. is an investigator of the Howard Hughes Medical Institute.

Received: February 24, 2012
Revised: April 3, 2012
Accepted: May 1, 2012
Published: June 21, 2012

REFERENCES

Bagri, A., Cheng, H.J., Yaron, A., Pleasure, S.J., and Tessier-Lavigne, M. (2003). Stereotyped pruning of long hippocampal axon branches triggered by retraction inducers of the semaphorin family. Cell *113*, 285–299.

Bashaw, G.J., and Klein, R. (2010). Signaling from axon guidance receptors. Cold Spring Harb. Perspect. Biol. *2*, a001941.

Beg, A.A., Sommer, J.E., Martin, J.H., and Scheiffele, P. (2007). alpha2-Chimaerin is an essential EphA4 effector in the assembly of neuronal locomotor circuits. Neuron *55*, 768–778.

Billuart, P., Winter, C.G., Maresh, A., Zhao, X., and Luo, L. (2001). Regulating axon branch stability: the role of p190 RhoGAP in repressing a retraction signaling pathway. Cell *107*, 195–207.

Buttery, P., Beg, A.A., Chih, B., Broder, A., Mason, C.A., and Scheiffele, P. (2006). The diacylglycerol-binding protein alpha1-chimaerin regulates dendritic morphology. Proc. Natl. Acad. Sci. USA *103*, 1924–1929.

Canagarajah, B., Leskow, F.C., Ho, J.Y., Mischak, H., Saidi, L.F., Kazanietz, M.G., and Hurley, J.H. (2004). Structural mechanism for lipid activation of the Rac-specific GAP, beta2-chimaerin. Cell *119*, 407–418.

Chen, H., Bagri, A., Zupicich, J.A., Zou, Y., Stoeckli, E., Pleasure, S.J., Lowenstein, D.H., Skarnes, W.C., Chédotal, A., and Tessier-Lavigne, M. (2000). Neuropilin-2 regulates the development of selective cranial and sensory nerves and hippocampal mossy fiber projections. Neuron *25*, 43–56.

Crusio, W.E., Schwegler, H., and Lipp, H.P. (1987). Radial-maze performance and structural variation of the hippocampus in mice: a correlation with mossy fibre distribution. Brain Res. *425*, 182–185.

Fernández-Chacón, R., Königstorfer, A., Gerber, S.H., García, J., Matos, M.F., Stevens, C.F., Brose, N., Rizo, J., Rosenmund, C., and Südhof, T.C. (2001). Synaptotagmin I functions as a calcium regulator of release probability. Nature *410*, 41–49.

Giger, R.J., Cloutier, J.F., Sahay, A., Prinjha, R.K., Levengood, D.V., Moore, S.E., Pickering, S., Simmons, D., Rastan, S., Walsh, F.S., et al. (2000). Neuropilin-2 is required in vivo for selective axon guidance responses to secreted semaphorins. Neuron *25*, 29–41.

Grosse, G., Tapp, R., Wartenberg, M., Sauer, H., Fox, P.A., Grosse, J., Gratzl, M., and Bergmann, M. (1998). Prenatal hippocampal granule cells in primary cell culture form mossy fiber boutons at pyramidal cell dendrites. J. Neurosci. Res. *51*, 602–611.

Hall, A., and Lalli, G. (2010). Rho and Ras GTPases in axon growth, guidance, and branching. Cold Spring Harb. Perspect. Biol. *2*, a001818.

Harrington, A.W., St Hillaire, C., Zweifel, L.S., Glebova, N.O., Philippidou, P., Halegoua, S., and Ginty, D.D. (2011). Recruitment of actin modifiers to TrkA endosomes governs retrograde NGF signaling and survival. Cell *146*, 421–434.

Hashimoto, R., Yoshida, M., Kunugi, H., Ozaki, N., Yamanouchi, Y., Iwata, N., Suzuki, T., Kitajima, T., Tatsumi, M., and Kamijima, K. (2005). A missense polymorphism (H204R) of a Rho GTPase-activating protein, the chimerin 2 gene, is associated with schizophrenia in men. Schizophr. Res. *73*, 383–385.

Holmes, G.L., Sarkisian, M., Ben-Ari, Y., and Chevassus-Au-Louis, N. (1999). Mossy fiber sprouting after recurrent seizures during early development in rats. J. Comp. Neurol. *404*, 537–553.

Hoopfer, E.D., McLaughlin, T., Watts, R.J., Schuldiner, O., O'Leary, D.D., and Luo, L. (2006). Wlds protection distinguishes axon degeneration following injury from naturally occurring developmental pruning. Neuron *50*, 883–895.

Ip, J.P., Shi, L., Chen, Y., Itoh, Y., Fu, W.Y., Betz, A., Yung, W.H., Gotoh, Y., Fu, A.K., and Ip, N.Y. (2011). α2-chimaerin controls neuronal migration and functioning of the cerebral cortex through CRMP-2. Nat. Neurosci. *15*, 39–47.

Iwasato, T., Katoh, H., Nishimaru, H., Ishikawa, Y., Inoue, H., Saito, Y.M., Ando, R., Iwama, M., Takahashi, R., Negishi, M., and Itohara, S. (2007). Rac-GAP alpha-chimerin regulates motor-circuit formation as a key mediator of EphrinB3/EphA4 forward signaling. Cell *130*, 742–753.

Johnston, M.V. (2004). Clinical disorders of brain plasticity. Brain Dev. *26*, 73–80.

Lakso, M., Pichel, J.G., Gorman, J.R., Sauer, B., Okamoto, Y., Lee, E., Alt, F.W., and Westphal, H. (1996). Efficient in vivo manipulation of mouse genomic sequences at the zygote stage. Proc. Natl. Acad. Sci. USA *93*, 5860–5865.

Lauder, J.M., and Mugnaini, E. (1977). Early hyperthyroidism alters the distribution of mossy fibres in the rat hippocampus. Nature *268*, 335–337.

Lee, T., Lee, A., and Luo, L. (1999). Development of the Drosophila mushroom bodies: sequential generation of three distinct types of neurons from a neuroblast. Development *126*, 4065–4076.

Lewis, D.A., and Levitt, P. (2002). Schizophrenia as a disorder of neurodevelopment. Annu. Rev. Neurosci. *25*, 409–432.

Lipp, H.P., Schwegler, H., Heimrich, B., and Driscoll, P. (1988). Infrapyramidal mossy fibers and two-way avoidance learning: developmental modification of hippocampal circuitry and adult behavior of rats and mice. J. Neurosci. *8*, 1905–1921.

Liu, X.B., Low, L.K., Jones, E.G., and Cheng, H.J. (2005). Stereotyped axon pruning via plexin signaling is associated with synaptic complex elimination in the hippocampus. J. Neurosci. *25*, 9124–9134.

Lois, C., Hong, E.J., Pease, S., Brown, E.J., and Baltimore, D. (2002). Germline transmission and tissue-specific expression of transgenes delivered by lentiviral vectors. Science *295*, 868–872.

Low, L.K., Liu, X.B., Faulkner, R.L., Coble, J., and Cheng, H.J. (2008). Plexin signaling selectively regulates the stereotyped pruning of corticospinal axons from visual cortex. Proc. Natl. Acad. Sci. USA *105*, 8136–8141.

Luo, L., and O'Leary, D.D. (2005). Axon retraction and degeneration in development and disease. Annu. Rev. Neurosci. *28*, 127–156.

McLaughlin, T., Torborg, C.L., Feller, M.B., and O'Leary, D.D. (2003). Retinotopic map refinement requires spontaneous retinal waves during a brief critical period of development. Neuron *40*, 1147–1160.

Miyake, N., Chilton, J., Psatha, M., Cheng, L., Andrews, C., Chan, W.M., Law, K., Crosier, M., Lindsay, S., Cheung, M., et al. (2008). Human CHN1 mutations hyperactivate alpha2-chimaerin and cause Duane's retraction syndrome. Science *321*, 839–843.

Nikolaev, A., McLaughlin, T., O'Leary, D.D., and Tessier-Lavigne, M. (2009). APP binds DR6 to trigger axon pruning and neuron death via distinct caspases. Nature *457*, 981–989.

Pardo, C.A., and Eberhart, C.G. (2007). The neurobiology of autism. Brain Pathol. *17*, 434–447.

Rapoport, J.L., Giedd, J.N., Blumenthal, J., Hamburger, S., Jeffries, N., Fernandez, T., Nicolson, R., Bedwell, J., Lenane, M., Zijdenbos, A., et al. (1999). Progressive cortical change during adolescence in childhood-onset schizophrenia. A longitudinal magnetic resonance imaging study. Arch. Gen. Psychiatry *56*, 649–654.

Sahay, A., Molliver, M.E., Ginty, D.D., and Kolodkin, A.L. (2003). Semaphorin 3F is critical for development of limbic system circuitry and is required in neurons for selective CNS axon guidance events. J. Neurosci. *23*, 6671–6680.

Schnütgen, F., Doerflinger, N., Calléja, C., Wendling, O., Chambon, P., and Ghyselinck, N.B. (2003). A directional strategy for monitoring Cre-mediated recombination at the cellular level in the mouse. Nat. Biotechnol. *21*, 562–565.

Siliceo, M., García-Bernal, D., Carrasco, S., Díaz-Flores, E., Coluccio Leskow, F., Teixidó, J., Kazanietz, M.G., and Mérida, I. (2006). Beta2-chimaerin provides a diacylglycerol-dependent mechanism for regulation of adhesion and chemotaxis of T cells. J. Cell Sci. *119*, 141–152.

Stanfield, B.B., O'Leary, D.D., and Fricks, C. (1982). Selective collateral elimination in early postnatal development restricts cortical distribution of rat pyramidal tract neurones. Nature *298*, 371–373.

Tran, T.S., Kolodkin, A.L., and Bharadwaj, R. (2007). Semaphorin regulation of cellular morphology. Annu. Rev. Cell Dev. Biol. *23*, 263–292.

Tran, T.S., Rubio, M.E., Clem, R.L., Johnson, D., Case, L., Tessier-Lavigne, M., Huganir, R.L., Ginty, D.D., and Kolodkin, A.L. (2009). Secreted semaphorins control spine distribution and morphogenesis in the postnatal CNS. Nature *462*, 1065–1069.

Vanderhaeghen, P., and Cheng, H.J. (2010). Guidance molecules in axon pruning and cell death. Cold Spring Harb. Perspect. Biol. *2*, a001859.

Wang, H., Yang, C., Leskow, F.C., Sun, J., Canagarajah, B., Hurley, J.H., and Kazanietz, M.G. (2006). Phospholipase Cgamma/diacylglycerol-dependent activation of beta2-chimaerin restricts EGF-induced Rac signaling. EMBO J. *25*, 2062–2074.

Watts, R.J., Hoopfer, E.D., and Luo, L. (2003). Axon pruning during Drosophila metamorphosis: evidence for local degeneration and requirement of the ubiquitin-proteasome system. Neuron *38*, 871–885.

Wegmeyer, H., Egea, J., Rabe, N., Gezelius, H., Filosa, A., Enjin, A., Varoqueaux, F., Deininger, K., Schnütgen, F., Brose, N., et al. (2007). EphA4-dependent axon guidance is mediated by the RacGAP alpha2-chimaerin. Neuron *55*, 756–767.

West, J.R., Hodges, C.A., and Black, A.C., Jr. (1981). Prenatal exposure to ethanol alters the organization of hippocampal mossy fibers in rats. Science *211*, 957–959.

Williams, M.E., Wilke, S.A., Daggett, A., Davis, E., Otto, S., Ravi, D., Ripley, B., Bushong, E.A., Ellisman, M.H., Klein, G., and Ghosh, A. (2011). Cadherin-9 regulates synapse-specific differentiation in the developing hippocampus. Neuron *71*, 640–655.

Xu, N.J., and Henkemeyer, M. (2009). Ephrin-B3 reverse signaling through Grb4 and cytoskeletal regulators mediates axon pruning. Nat. Neurosci. *12*, 268–276.

Yang, C., and Kazanietz, M.G. (2007). Chimaerins: GAPs that bridge diacylglycerol signalling and the small G-protein Rac. Biochem. J. *403*, 1–12.

Zhou, Z., Hong, E.J., Cohen, S., Zhao, W.N., Ho, H.Y., Schmidt, L., Chen, W.G., Lin, Y., Savner, E., Griffith, E.C., et al. (2006). Brain-specific phosphorylation of MeCP2 regulates activity-dependent Bdnf transcription, dendritic growth, and spine maturation. Neuron *52*, 255–269.